Check for updates

Feedback Regulation between Aquatic Microorganisms and the Bloom-Forming Cyanobacterium *Microcystis aeruginosa*

Meng Zhang,[a] Tao Lu,[a] Hans W. Paerl,[b,c] Yiling Chen,[d] Zhenyan Zhang,[a] Zhigao Zhou,[a] Haifeng Qian[a]

[a]College of Environment, Zhejiang University of Technology, Hangzhou, People's Republic of China
[b]Institute of Marine Sciences, University of North Carolina at Chapel Hill, Morehead City, North Carolina, USA
[c]College of Environment, Hohai University, Nanjing, People's Republic of China
[d]Department of Civil, Environmental, and Geo-Engineering, University of Minnesota, Minneapolis, Minnesota, USA

ABSTRACT The frequency and intensity of cyanobacterial blooms are increasing worldwide. Interactions between toxic cyanobacteria and aquatic microorganisms need to be critically evaluated to understand microbial drivers and modulators of the blooms. In this study, we applied 16S/18S rRNA gene sequencing and metabolomics analyses to measure the microbial community composition and metabolic responses of the cyanobacterium *Microcystis aeruginosa* in a coculture system receiving dissolved inorganic nitrogen and phosphorus (DIP) close to representative concentrations in Lake Taihu, China. *M. aeruginosa* secreted alkaline phosphatase using a DIP source produced by moribund and decaying microorganisms when the P source was insufficient. During this process, *M. aeruginosa* accumulated several intermediates in energy metabolism pathways to provide energy for sustained high growth rates and increased intracellular sugars to enhance its competitive capacity and ability to defend itself against microbial attack. It also produced a variety of toxic substances, including microcystins, to inhibit metabolite formation via energy metabolism pathways of aquatic microorganisms, leading to a negative effect on bacterial and eukaryotic microbial richness and diversity. Overall, compared with the monoculture system, the growth of *M. aeruginosa* was accelerated in coculture, while the growth of some cooccurring microorganisms was inhibited, with the diversity and richness of eukaryotic microorganisms being more negatively impacted than those of prokaryotic microorganisms. These findings provide valuable information for clarifying how *M. aeruginosa* can potentially modulate its associations with other microorganisms, with ramifications for its dominance in aquatic ecosystems.

IMPORTANCE We measured the microbial community composition and metabolic responses of *Microcystis aeruginosa* in a microcosm coculture system receiving dissolved inorganic nitrogen and phosphorus (DIP) close to the average concentrations in Lake Taihu. In the coculture system, DIP is depleted and the growth and production of aquatic microorganisms can be stressed by a lack of DIP availability. *M. aeruginosa* could accelerate its growth via interactions with specific cooccurring microorganisms and the accumulation of several intermediates in energy metabolism-related pathways. Furthermore, *M. aeruginosa* can decrease the carbohydrate metabolism of cooccurring aquatic microorganisms and thus disrupt microbial activities in the coculture. This also had a negative effect on bacterial and eukaryotic microbial richness and diversity. Microcystin was capable of decreasing the biomass of total phytoplankton in aquatic microcosms. Overall, compared to the monoculture, the growth of total aquatic microorganisms is inhibited, with the diversity and richness of eukaryotic microorganisms being more negatively impacted than those of prokaryotic microorganisms. The only exception is *M. aeruginosa* in the coculture system, whose growth was accelerated.

KEYWORDS *Microcystis aeruginosa*, aquatic microcosm, 16S/18S rRNA gene sequencing, metabolomics analyses, cocultures

Anthropogenic nutrient enrichment and climatic changes, as well as exotic species invasions, can induce dramatic disturbances and regime shifts in ecosystems (1, 2). In aquatic ecosystems, the emergence of cyanobacterial harmful algal blooms (CyanoHABs) during the transition from oligotrophic to eutrophic conditions represents a regime shift, as indicated by changes in dominant microbes and new combinations of various microbial communities. CyanoHABs, especially *Microcystis* blooms, pose a major threat to freshwater ecosystems globally by altering food webs, creating hypoxic zones, and producing secondary metabolites (i.e., "cyanotoxins") that can negatively impact biota ranging from aquatic macrophytes to invertebrates, fish, and mammals, including humans (3, 4).

Cyanobacteria are among the most ancient living organisms on Earth (originating ~3 billion years ago). Their diverse and flexible metabolic capabilities enable them to adapt to major environmental changes (3). Essential nutrients such as nitrogen (N) and phosphorus (P) play key roles in supporting cyanobacterial production and composition in freshwater systems (5, 6). However, excessive inputs of nutrients can promote the development and proliferation of CyanoHABs (3, 7), especially with increasing water temperature (8). The frequency, intensity, and duration of cyanobacterial blooms in many aquatic ecosystems globally are linked to accelerating eutrophication. Recent studies have shown that reductions in both P and N inputs are essential for controlling blooms (9–12). Moreover, studies have shown that *Microcystis* is capable of scavenging dissolved organic phosphorus (DOP), thereby providing a source of P under dissolved inorganic phosphorus (DIP)-depleted conditions (6).

Secondary metabolites produced by *Microcystis* (microcystins [MCs], micropeptins, linoleic acid, etc.) have been shown to be toxic to some biota (13–15). For example, *Microcystis* is capable of inhibiting photosynthesis, carbon metabolism, and amino acid metabolism in *Chlorella pyrenoidosa* via the production of linoleic acid (16). In addition, the microbial community associated with CyanoHABs is different from that under nonbloom conditions (17, 18). *Microcystis* blooms strongly affect eukaryotic abundance (13, 17). Field studies in Lake Taihu, the third largest freshwater lake in China, have shown that blooms had a negative effect on bacterial diversity and richness (19, 20). Zooplankton (including crustaceans, rotifers, and protozoa) has a limited ability to ingest cyanobacteria, especially colonial and filamentous genera. Meanwhile, some cyanobacterial secondary metabolites can also be toxic to zooplankton. These constraints can negatively impact the transfer of cyanobacterial biomass to higher trophic levels (21, 22). Furthermore, some cyanobacterial genera can fix atmospheric N, thereby providing biologically available N on an ecosystem scale (23). Some bacteria attach to cyanobacterial cells, and they can grow on extracellular mucus or form free-living populations (24, 25). Overall, there is renewed interest in how *Microcystis aeruginosa* and aquatic microorganisms interact under various nutritional conditions.

In this study, we utilized a laboratory coculture system in which a dialysis membrane was used to separate *M. aeruginosa* and aquatic microorganisms in a microcosm, allowing their growth in an isolated culture and exchange of excretion products. The system allowed for measurements of physicochemical water quality parameters (detailed in Materials and Methods), cell enumeration, microbial composition and diversity (high-throughput sequencing data sets, including 16S and 18S rRNA gene sequencing), and metabolomics analysis to address the interactions between *M. aeruginosa* and the native microbial community.

RESULTS AND DISCUSSION

***M. aeruginosa* and microbial growth states.** According to Fig. 1B, the optical density at 680 nm (OD_{680}) and the amount of *M. aeruginosa* cells in the Treat-Ma group (i.e., treatment with *M. aeruginosa*) were significantly higher than those in the Con-Ma group (i.e., the *M. aeruginosa* control group) after 3 days of coculture. However, the OD_{680} and chlorophyll *a* (Chl-a) levels in the Treat-AM group (i.e., treatment with aquatic microorganisms) were significantly lower than those in the Con-AM group (Fig. 1C). Figure S2 in the supplemental material also shows that the turbidity of the medium changed in coculture microcosms (more transparent) compared to that of Con-AM after
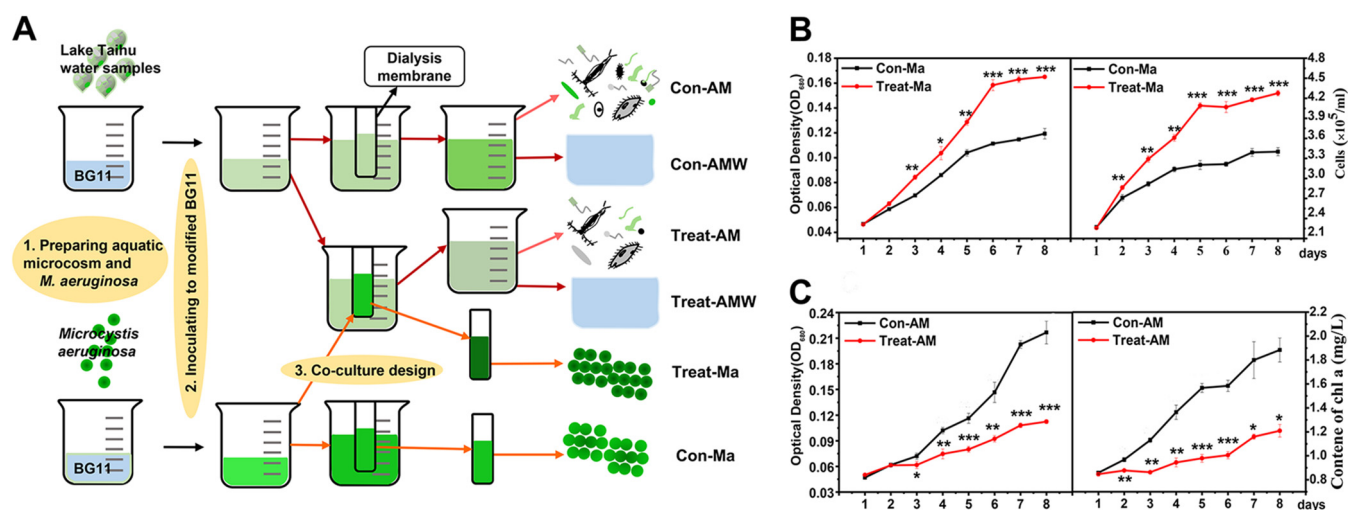
FIG 1 Design of the experiment and the growth tendency of *M. aeruginosa* and aquatic microorganisms in monoculture and coculture. (A) Experimental flow chart. (B) Optical density (OD_{680}) and cell number of *M. aeruginosa*. (C) Optical density (OD_{680}) and chlorophyll *a* (Chl-a) of aquatic microcosms. Asterisks (*, **, and ***) represent statistically significant differences compared to the control ($P < 0.05$, $P < 0.01$, and $P < 0.001$, respectively; $n = 3$).

8 days of culture, indicating that the growth of cooccurring microorganisms was inhibited in the coculture system.

In addition, the dissolved oxygen (DO) and pH values were significantly lower during the coculture process in the Treat-AM group than in the Con-AM group (i.e., the aquatic organism control group) (Fig. 2). Dense *Microcystis* populations can consume oxygen through respiration at night and through microbial decomposition of moribund cells, resulting in an insufficient oxygen supply in the water to support aerobic microbes and higher organisms (26, 27). An increase in the concentration of carbon dioxide shifts the inorganic carbon equilibrium away from carbonate and toward bicarbonate, decreasing the pH, which in turn inhibits the growth of some microbial populations (28). Furthermore, *Microcystis* inhibited some microorganisms, and the decomposition of these
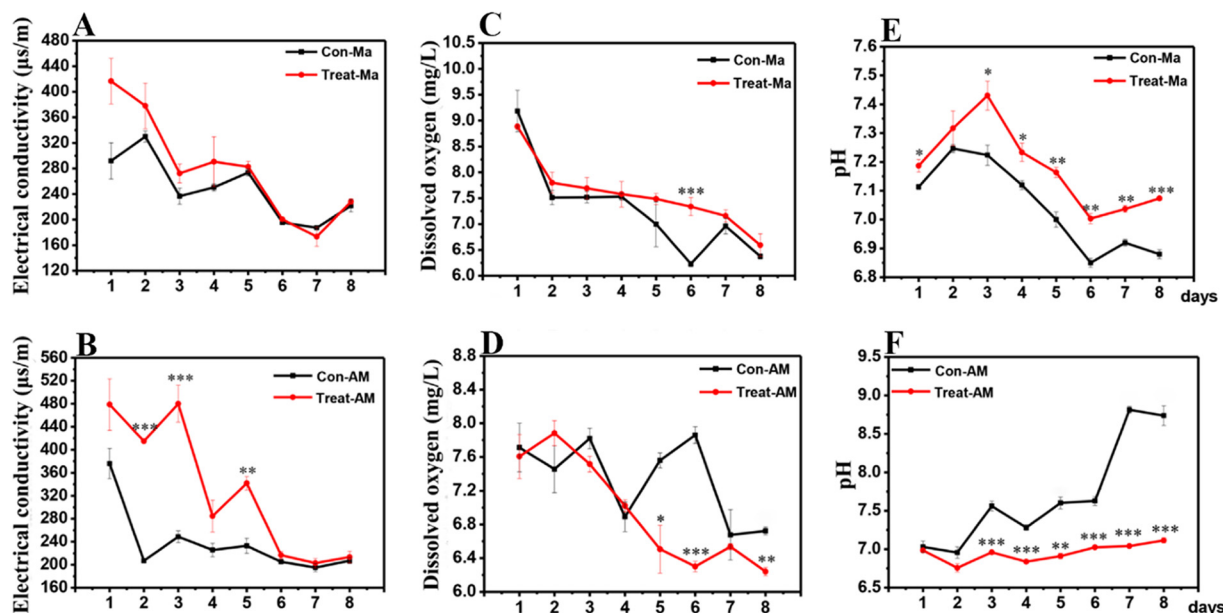

FIG 2 Water quality parameters of monocultures and cocultures in *M. aeruginosa* and aquatic microcosms. (A to F) Electrical conductivity (A and B), dissolved oxygen concentrations (C and D), and pH (E and F) in *M. aeruginosa* and aquatic microcosms. Asterisks (*, **, and ***) represent statistically significant differences compared to the control ($P < 0.05$, $P < 0.01$, and $P < 0.001$, respectively; $n = 3$). Panels A, C, and E show data for the Con-Ma/Treat-Ma groups, and panels B, D, and F show data for the Con-AM/Treat-AM groups.
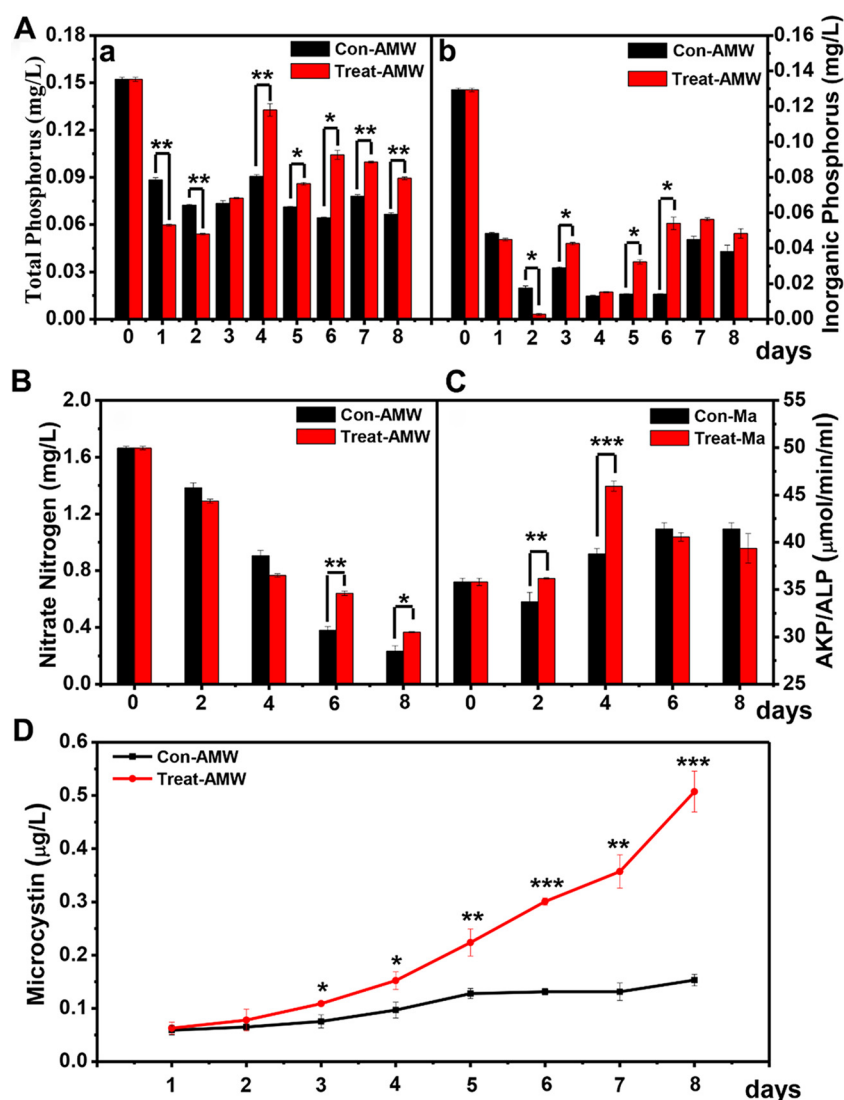
FIG 3 (A) Changes in total phosphorus (TP) and inorganic phosphorus (IP) in culture medium. (B) Changes in the nitrate nitrogen (NO_3^--N) concentration in culture medium. (C) Changes in the alkaline phosphatase (AKP) concentration in *Microcystis aeruginosa* cells. Asterisks (*, **, and ***) represent statistically significant differences compared to the control ($P < 0.05$, $P < 0.01$, and $P < 0.001$, respectively; $n = 3$). (D) Changes in the microcystin (MC) concentration in culture medium.

moribund cells would lead to an increase in oxygen consumption in the Treat-AM group (Fig. 2D). The electrical conductivity (EC) of each group was investigated as a function of the types and quantities of dissolved materials (29). Compared to the Con-AM group, the Treat-AM group showed an apparent increase in EC after 3 and 6 days of coculture. Notably, these water quality parameters (Fig. 2) especially the pH values, were significantly different between monoculture and coculture systems, suggesting that these physiochemical changes in the water were influenced by the metabolism of *M. aeruginosa* directly or indirectly, as well as by the associated microbial community.

Changes in N and P and MCs released in culture medium. Nitrogen and phosphorus availability are key factors controlling primary production and CyanoHAB dynamics (12). In this study, the concentrations of total phosphorus (TP) and DIP in coculture medium were lower than those in monoculture medium after 1 and 2 days of coculture, whereas the concentrations of TP and DIP in coculture medium were higher than those in monoculture medium after 3 to 8 days of coculture (Fig. 3A).

TABLE 1 16S alpha diversity in prokaryotic communities after 4 and 8 days of coculture (Treat-AM4 and Treat-AM8) and monoculture (Con-AM4 and Con-AM4)

Sample	Mean alpha diversity ± SEM[a]					
	Observed species	Shannon	Simpson	ACE	Chao1	Good's coverage
Con-AM4	303 ± 25[A]	3.11 ± 0.08[AB]	0.71 ± 0.01[AB]	393 ± 25[A]	396 ± 27[A]	0.99 ± 0.00[A]
Treat-AM4	282 ± 52[AB]	3.19 ± 0.23[A]	0.73 ± 0.02[A]	353 ± 64[A]	360 ± 64[A]	0.99 ± 0.00[A]
Con-AM8	247 ± 25[AB]	2.80 ± 0.04[AB]	0.65 ± 0.01[AB]	323 ± 37[A]	319 ± 30[A]	0.99 ± 0.00[A]
Treat-AM8	197 ± 10[B]	2.55 ± 0.27[B]	0.63 ± 0.05[B]	306 ± 7[A]	297 ± 18[A]	0.99 ± 0.00[A]

[a]Different superscript letters represent significant differences within one index ($P < 0.05$; $n = 3$).

Numerous algal species can synthesize alkaline phosphatase (AKP) to hydrolyze DOP to DIP when the TP is too low to satisfy algal growth demand (6). Consistent with previous studies (30), AKP in the Treat-Ma group increased dramatically after 2 and 4 days of coculture, whereas the AKP decreased with an increase in DIP (Fig. 3C). These results suggest a strong ability of *M. aeruginosa* to scavenge DOP from metabolic products released by organisms (6). With the active growth of *M. aeruginosa*, the nitrate nitrogen (NO_3^--N) level in the coculture system was also much higher than that in the monoculture system (Fig. 3B). This was due to the negative effect of *M. aeruginosa* on the growth of some accompanying species in the cocultured systems, leading to the release of nitrogen sources from moribund cells, while the reduction of aquatic microorganisms also decreased the consumption of nitrogen sources. This released N provided a readily available N source for *M. aeruginosa* growth, which might partly explain why *M. aeruginosa* growth in coculture is better than that in monoculture. There are likely multiple reasons why *Microcystis* growth is better in coculture, including the exchange of mutually beneficial metabolites (such as vitamins), CO_2 replenishment, and the exchange of nutrients and essential metals (31).

During coculture, *M. aeruginosa* exhibited more rapid growth relative to monocultures and produced a large number of MCs that were released into the culture medium. After 3 days of coculture, the MCs in Treat-AMW (culture medium in the treated group) were significantly higher than those in Con-AMW (culture medium in the control group) (Fig. 3D). Numerous studies have shown that MCs are toxic to some microorganisms (32). Our data also indicated that MCs caused a decrease in total phytoplankton in aquatic microcosms (see Fig. 7a).

Changes in bacterial community structure and diversity in aquatic microcosms under coculture conditions. Community diversity was calculated at the operational taxonomic unit (OTU) level. The Shannon and Simpson indices reflect the diversity and evenness of the community. Meanwhile, the ACE and Chao1 indices reflect the richness, which indicates the estimated number of species present (33). Compared to the Con-AM group, the Treat-AM group showed a downward trend in ACE and Chao1 indices at 4 and 8 days, and the Shannon and Simpson diversity indices also slightly decreased at 8 days in the Treat-AM group (Table 1), indicating a decline in the richness and diversity of bacterial communities. Table 1 indicates the numbers of observed species contained in the samples. Higher values of observed species in the Con-AM group also indicated a higher species richness than in the Treat-AM group. Changes in dominant cyanobacterial biomass affect the composition and function of microbial populations, whereas competitive exclusion tends to reduce the abundance of other, more readily grazed primary producers during cyanobacterial blooms (3, 4). Principal-component analysis (PCoA) showed that PC1 (first principal component) and PC2 (second principal component) explained 83.89% of the beta diversity (Fig. 4A) in the variation of species composition on the temporal scales. Coculture treatment could constitute a major portion of PC1, since it might result in the separation of the Con-AM and Treat-AM samples after 4 and 8 days of culture. Environmental factors such as nutritional status, pH, and predation might constitute PC2, which affects the OTU composition at certain times in culture (from 4 to 8 days). As shown in Fig. 4B, the eigenvalues of the first two redundancy analysis (RDA) axes explained 67.42% of the
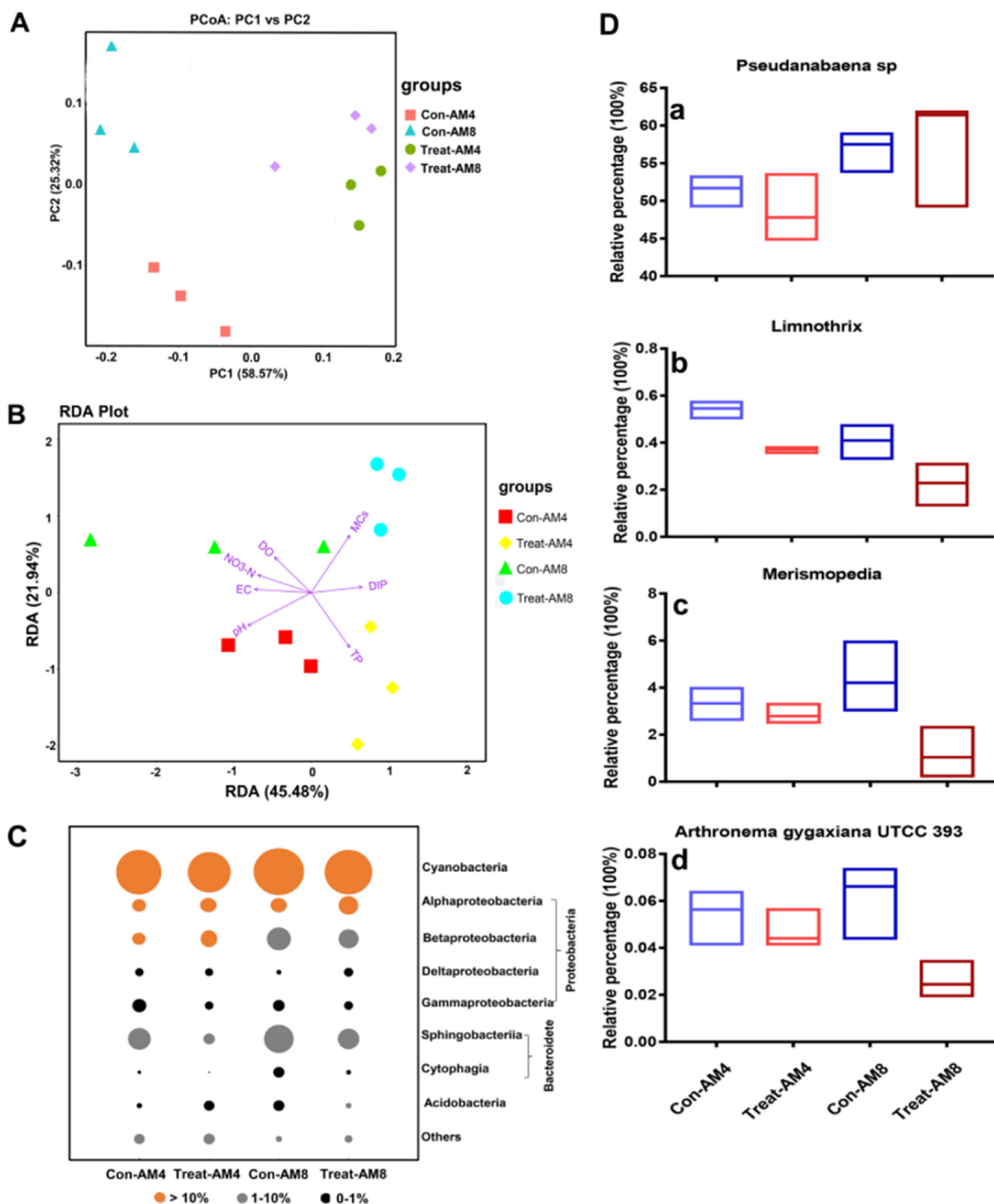
FIG 4 (A and B) Relative abundance of the 16S rRNA gene of the PCoA plot (A) and RDA ordination diagram of the data (B), with environmental variables represented by arrows and samples represented by different colors. (C) Main prokaryotic class of the bacterial communities after 4 and 8 days of coculture (Treat-AM4 and Treat-AM8) and monoculture (Con-AM4 and Con-AM8). (D) The four most-abundant taxa in *Cyanobacteria* after 4 and 8 days of coculture (Treat-AM4 and Treat-AM8) and monoculture (Con-AM4 and Con-AM8) in aquatic microcosms. Each group had three biological replicates.

TABLE 2 18S alpha diversity in eukaryotic communities after 4 and 8 days of coculture (Treat-AM4 and Treat-AM8) and monoculture (Con-AM4 and Con-AM4)

Sample	Mean alpha diversity ± SEM[a]					
	Observed species	Shannon	Simpson	ACE	Chao1	Good's coverage
Con-AM4	46 ± 1[A]	2.28 ± 0.03[A]	0.76 ± 0.00[A]	56 ± 4[A]	396 ± 27[A]	0.99 ± 0.00[A]
Treat-AM4	25 ± 1[B]	1.98 ± 0.04[B]	0.68 ± 0.01[BD]	29 ± 2[BC]	360 ± 64[A]	0.99 ± 0.00[A]
Con-AM8	34 ± 4[C]	2.14 ± 0.04[C]	0.71 ± 0.01[C]	39 ± 4[B]	319 ± 30[A]	0.99 ± 0.00[A]
Treat-AM8	26 ± 2[BC]	1.77 ± 0.04[D]	0.67 ± 0.01[BD]	28 ± 1[C]	297 ± 18[A]	0.99 ± 0.00[A]

[a]Different superscript letters represent significant differences within one index ($P < 0.05$; $n = 3$).

total variation. The RDA scores showed strong relationships between the environmental variables and the four groups. Samples of Con-AM4 and Con-AM8 were positively correlated with EC, DO, pH, and NO_3^--N. The Treat-AM8 and Treat-AM8 groups clustered together and showed the highest correlation with MCs and DIP.

Bacterial community analysis revealed that the microbial community in the microcosms at the class level was dominated by *Cyanobacteria*, *Alphaproteobacteria*, *Betaproteobacteria*, and *Sphingobacteria* at both 4 and 8 days of coculture and monoculture (Fig. 4C), whereas other classes did not exceed 1%. In both cocultures and monocultures, *Cyanobacteria* (>50%) was the dominant class of abundance, and the top four taxa of abundance among the *Cyanobacteria* were *Pseudanabaena*, *Merismopedia*, *Limnothrix*, and *Arthronema gygaxiana* UTCC 393 in aquatic microcosms at 4 and 8 days (Fig. 4D). Interestingly, the abundance of *Cyanobacteria* in the aquatic microcosms was significantly lower in the Treat-AM8 group than in the Con-AM8 group, except for *Pseudanabaena*. The growth of some freshwater bacteria has been reported to be associated with cyanobacterial blooms, but phytoplankton species are mainly conserved at the phylum level in *Proteobacteria*, *Bacteroidetes* and *Actinobacteria* (34). After coculture with *M. aeruginosa*, the *Alphaproteobacteria* and *Betaproteobacteria* significantly increased, whereas the *Sphingobacteria* decreased, indicating that the abundance of some bacteria is affected by an increase in *M. aeruginosa* biomass. Moreover, coculture with *M. aeruginosa* disturbed the composition of rare microorganisms (relative abundance < 1%). Hundreds of rare microorganisms decreased in relative abundance or disappeared after 8 days in coculture (see Data Set S1 in the supplemental material).

Changes in eukaryotic microorganism community structure and diversity in aquatic microcosms cocultured with *M. aeruginosa*. The decrease in species diversity and richness from the Con-AM4 to the Con-AM8 group indicated a decline in eukaryotes over time (Table 2). The species diversity and richness from the Treat-AM group at 4 to 8 days did not show a downward trend; however, compared to the Con-AM group, the Treat-AM group at 4 and 8 days showed a downward trend in both ACE and Chao1 indices of eukaryotic microorganisms and in Shannon and Simpson diversity indices. These findings indicate that coculture reduces the diversity and richness of eukaryotic species. PCoA showed that PC1 and PC2 explained 92.03% of the beta diversity (Fig. 5A). The coordinates of the Con-AM4 and Treat-AM4 groups were separated by PC1, and the Con-AM8 and Treat-AM8 groups were affected more severely by PC2. Changes in the 4-day cocultures may be affected by *M. aeruginosa*, and the changes in physicochemical water quality parameters, such as pH and dissolved oxygen, may be related to 8-day cocultures.

In the eukaryotic community, diverse species were identified, including some chromista such as Ciliophora and Ochrophyta; metazoans such as Rotifera; viridiplantae such as Streptophyta; and fungi such as Cryptomycota, Ascomycota, and Dikarya (Fig. 5B). There are interrelationships between eukaryotes in areas such as predation, competitive relationships, and parasitism (25). In monocultures, Rotifera was the most abundant eukaryotic taxon, accounting for 29.88 and 43.81% of the eukaryotic sequences of the Con-AM group at 4 and 8 days, respectively. Rotifers are usually very active grazers, affecting phytoplankton biomass and richness in the Con-AM group. Compared to the Con-AM group, the Treat-AM group showed a reduction in the relative abundance of Rotifera to 8.00 and 23.45% after 4 and 8 days of coculture, respectively, and Ciliophora became the most abundant eukaryote in cocultures. As consumers, Rotifera and Ciliophora are correlated in predation
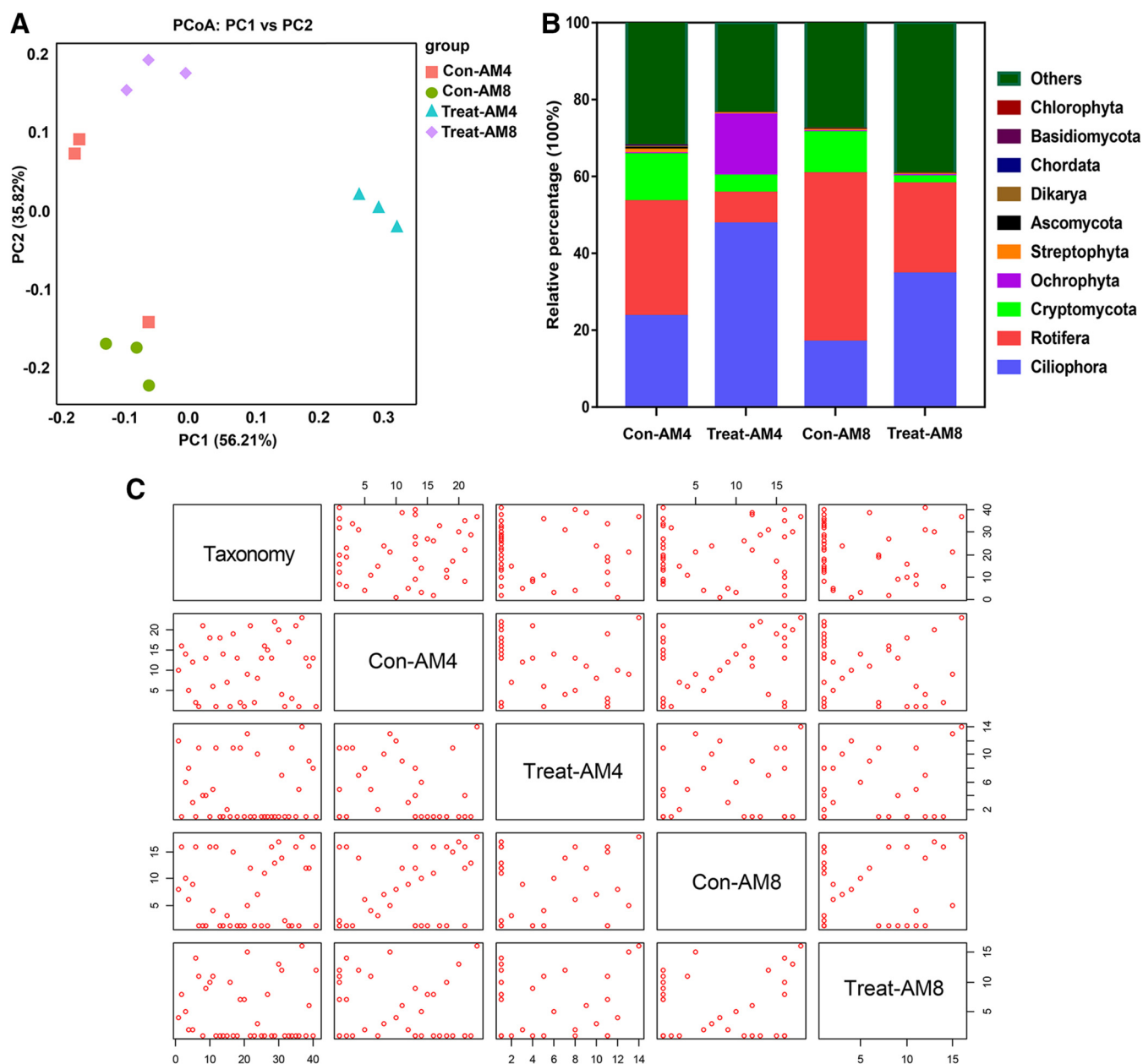
FIG 5 (A and B) Relative abundance of the 18S rRNA gene of PCoA plot (A) and main eukaryotic phylum of the microbial communities after 4 and 8 days of coculture (Treat-AM4 and Treat-AM8) and monoculture (Con-AM4 and Con-AM8) (B). (C) Scattered atlas of rare microorganisms (the taxonomy represents rare microorganism species). The figure is symmetric along the diagonal, and each dot in the graph represents a rare microbial genus. The first row and the first column represent the distribution of rare microorganisms. The genus near the axis has the lowest relative abundance. The remaining rows or columns represent the comparison between the two groups. Each group had three biological replicates.

and nutrition competition experiments (35). Our study showed that toxic blooms have greater impacts on the composition of these active grazers and therefore change their food (aquatic microorganism) items. In contrast, other eukaryotes such as Cryptomycota, Streptophyta, Ascomycota, and Chordata decreased after coculture. In addition, rare microorganisms moved closer to the coordinate axis in the Treat-AM4 and Treat-AM8 groups compared to those in the Con-AM4 and Con-AM8 groups, suggesting the decrease or complete disappearance of the rare microorganisms (Fig. 5C). The synergistic effects between rare and common taxa may play central roles in maintaining the stability of the eukaryotic community and its ecological function (36).

Metabolic responses of *M. aeruginosa* and aquatic microcosms in cocultures and monocultures. To clarify the mechanisms underlying the effect of *M. aeruginosa*
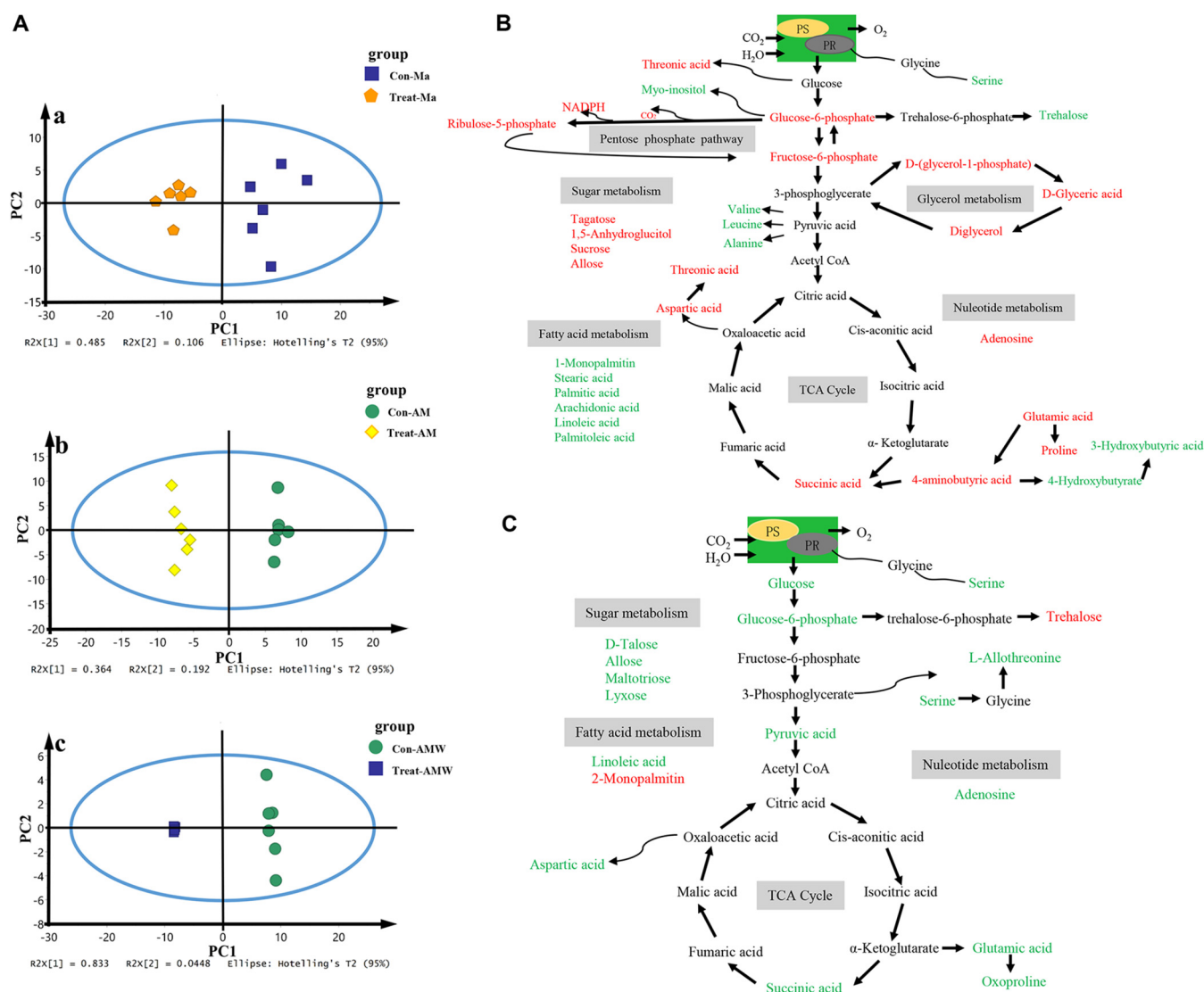
FIG 6 (A) Principal-component analysis (PCoA) of intracellular *M. aeruginosa* metabolites, cellular microorganisms, and culture medium after 8 days of coculture and monoculture. (B and C) Schematic diagrams of proposed metabolic pathways in cellular *M. aeruginosa* metabolites (B) and cellular microorganisms (C) after 8 days of coculture and monoculture. Red and green represent up- and downregulated metabolites, respectively. Each group had six biological replicates. PR, photorespiration; PS, photosynthesis.

on the microcosm community, we measured metabolite changes in *M. aeruginosa* and microcosms. A total of 239 metabolites were identified. The score plot of PCoA and partial least-squares discriminant analysis (PLS-DA) showed noticeable separation between cocultures and monocultures from *M. aeruginosa* and the microcosm along PC1 (Fig. 6A and Fig. S3). In multivariate statistical analysis, screening and determining the difference variables were performed by calculating the variable importance (VIP) between groups. VIP, which is the weighted sum of squares of the PLS-DA, indicates the importance of a variable to the entire model (37). A variable with a VIP of >1 is regarded as responsible for separation, defined as a discriminating metabolite in this study. In a univariate statistical analysis, the *P* value was used to assess the statistical significance of difference variables. We combined these two criteria to screen variables with a VIP of >1 and a *P* value of <0.05 as difference variables. Significant metabolite changes were observed for *M. aeruginosa* (53 downregulated and 31 upregulated [Table S2]), aquatic microorganisms from microcosms (39 downregulated and 18 upregulated [Fig. S4]), and culture medium samples (53 downregulated [Table S3] and S10 upregulated [Table 3]), respectively.

TABLE 3 Metabolic profile changes in culture medium samples of microcosms

Candidate metabolite[a]	VIP value[b]	Fold change	P
Phenaceturic acid	1.00448	∞	3.12E–05
Monoolein	1.03266	∞	4.73E–06
3,6-Anhydro-D-galactose	1.05576	∞	6.23E–07
Dihydroxyacetone	1.06905	∞	8.77E–08
D-Glyceric acid	1.06959	∞	8.71E–08
L-Threose	1.07709	∞	1.34E–08
Fucose	1.08395	∞	1.86E–09
Thymidine	1.09358	∞	9.58E–13
Diglycerol	1.09455	∞	1.38E–13
Glycerol	1.09643	11.02	4.84E–18

[a]All of the metabolites were upregulated.
[b]VIP represents variable importance.

Metabolic profiles and pathway changes in *M. aeruginosa* and aquatic microcosms in cocultures and monocultures. The components of the pentose phosphate (PP) pathway or glycolysis intermediates, such as glucose-6-phosphate (G6P), fructose-6-phosphate (F6P), and ribulose-5-phosphate (Ru5P), significantly increased in the Treat-Ma group (Fig. 6B) relative to the Con-Ma group. G6P and F6P are interconnected through biochemical reactions with the Calvin cycle to glycogen biosynthesis for energy expenditure (38, 39). Their accumulation played an active role in the growth of *M. aeruginosa*, which indicated that the carbon fixation in *M. aeruginosa* cells was enhanced by the coculture treatment. Succinic acid, an intermediate in the tricarboxylic acid (TCA) cycle, was 18.30-fold higher in the Treat-Ma group than in the Con-Ma group. These increased intermediates in the PP pathway, glycolysis, and the TCA cycle could provide precursors for amino acid synthesis and the transfer of other cellular macromolecules (40, 41). They are also beneficial in the generation of reducing power (NADPH and NADH) and energy (ATP) for AKP and MC synthesis and cell growth. The AKP synthesis in *M. aeruginosa* implied the manifestation of cellular responses to stress (6), specifically the hydrolysis of DOP to support *M. aeruginosa* growth under low-DIP conditions. Higher metabolite levels accelerate *M. aeruginosa* growth, with that organism forming aggregates that are dominant in competition with microbes and produce various toxic substances that inhibit the growth of other microbes. This conclusion is illustrated in Fig. 1B and 3D, which show that the growth of *M. aeruginosa* in a coculture system was faster than that in a monoculture, and a large amount of MCs was produced. Overall, the upregulation of these pathways in *M. aeruginosa* was beneficial for the production of MCs, AKP, and energy, thus enhancing the competitive capacity and defensive ability of *M. aeruginosa*.

Sugars participate in energy metabolism, playing critical roles as signaling molecules (37) or as osmoprotectants (42). A significant increase in a compatible solute ($P \leq 0.05$) such as tagatose, 1,5-anhydroglucitol, sucrose, or allose in the Treat-Ma group during coculture decreased the water potential inside the cells to maintain osmotic pressure to avoid dehydration, such as during salt stress (42).

Compared to monoculture, coculture decreased the levels of several fatty acids in *M. aeruginosa*, such as 1-monopalmitin (0.76-fold), stearic acid (0.63-fold), palmitic acid (0.60-fold), and arachidonic acid (0.51-fold). Fatty acids and sterols with phospholipids are the primary components of the plasma membrane (43). Phospholipids are composed of polar head groups, glycerides, and two fatty acyl chains. Glycerol metabolism, which is related to the polar head group component of phospholipid, significantly ($P \leq 0.05$) increased upon exposure to coculture. These findings support the hypothesis that *M. aeruginosa* adjusts its membrane composition to maintain membrane integrity, and an increase in the cell division of *M. aeruginosa* alters intracellular metabolism to rebuild membrane integrity.

Amino acids play important roles in cyanobacterial physiological processes by acting as osmolytes, serving as precursors for the synthesis of defense-related metabolites and signaling molecules (44). Therefore, knowledge of these roles contributed to a holistic understanding of cyanobacteria against stress (45). The numbers of amino acids,
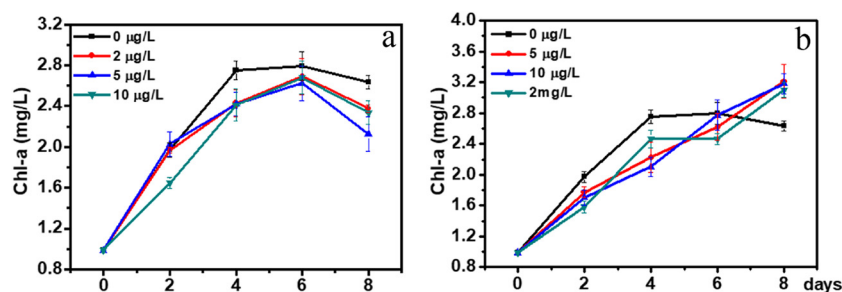
FIG 7 Chl-a content in aquatic microcosms with monoculture exposed to 0 to 10 μg/liter microcystin (a) or 0 to 2 mg/liter D-glyceric acid (b) for different periods of time.

including hydroxylamine (0.71-fold), norleucine (0.83-fold), N-methyl-D,L-alanine (0.71-fold), and alanine (0.72-fold), were lower in the Treat-Ma group than in the Con-Ma group. We postulated that the decrease in amino acids (containing N elements) in the Treat-Ma group was caused by the acceleration of protein synthesis to satisfy the growth of *M. aeruginosa*. Aspartate, which can be synthesized by microorganisms via TCA cycle intermediates, is an important substrate for microcystin biosynthesis in *M. aeruginosa* (46, 47). An increase in aspartate in the Treat-Ma group may contribute to the overproduction of microcystin (Fig. 3D).

In microcosms, several intermediates involved in energy metabolism pathways, such as glycolysis, the TCA cycle, and sugar metabolism, decreased after coculture in the Treat-AM group (Fig. 6C). The reduction of these intermediates could be attributed to the reduced defensive ability of aquatic microorganisms caused by negative environmental factors (pH, DO, MCs, and DIP). This finding is also consistent with the decrease in Chl-a in the aquatic microcosm after coculture.

Interspecies network of interactions. At the metabolomics level, the contents of the following metabolites particularly increased in the Treat-AM group: D-glyceric acid (1.78-fold), monoolein (1.63-fold), and diglycerol (1.63-fold; Table S2). Furthermore, the concentrations of monoolein, D-glyceric acid, diglycerol, and MCs (independently analyzed by a Beacon MC plate kit [Beijing Ease Century Trade Co., Ltd., Beijing, China]) in coculture medium were higher than those in monoculture medium (Table 3), demonstrating that these compounds were secreted by *M. aeruginosa*. Monoolein is nontoxic and biodegradable, while diglycerol can be bioavailable as a carbon source (48, 49). To verify their potential allelopathic roles, MCs and D-glyceric acid were added into separate monoculture microcosms. The Chl-a content decreased with the presence of MCs in aquatic microcosms but remained constant with glyceric acid (Fig. 7), implying that MCs play a role in the decrease in total phytoplankton in microcosms. We were unable to verify whether MCs could change the original cultured microbial community. However, MCs caused a decrease in total phytoplankton in microcosms. MCs appear to be toxic to some nearby organisms, and the binding of MCs may protect cyanobacterial proteins from oxidative stress to enhance the viability of cyanobacteria (27, 50). In addition to the upregulation of metabolites, the downregulation of various substances (such as glucose-1-phosphate, malonic acid, and carnitine) metabolized by *M. aeruginosa* or aquatic microorganisms was more obvious in coculture medium (Treat-AMW/Con-AMW ≤ 0.28, Table S3). The downregulation of these substances may also affect the growth of aquatic microorganisms in cocultures compared to that in monocultures.

A schematic diagram of changes in *M. aeruginosa* and microbial communities after coculture treatment is shown in Fig. 8. Our study demonstrated that *M. aeruginosa* can secrete AKP, making DOP produced by dying and decaying microorganisms available when the P source is insufficient. At the same time, *M. aeruginosa* produces a variety of toxic substances such as MCs, inhibiting some key intermediates accumulating in energy metabolism pathways (such as glycolysis, the TCA cycle, and sugar metabolism) in aquatic microorganisms and thus inhibiting microbial growth. *M. aeruginosa* produced MCs, AKP, and energy to enhance its competitive capacity and defensive ability
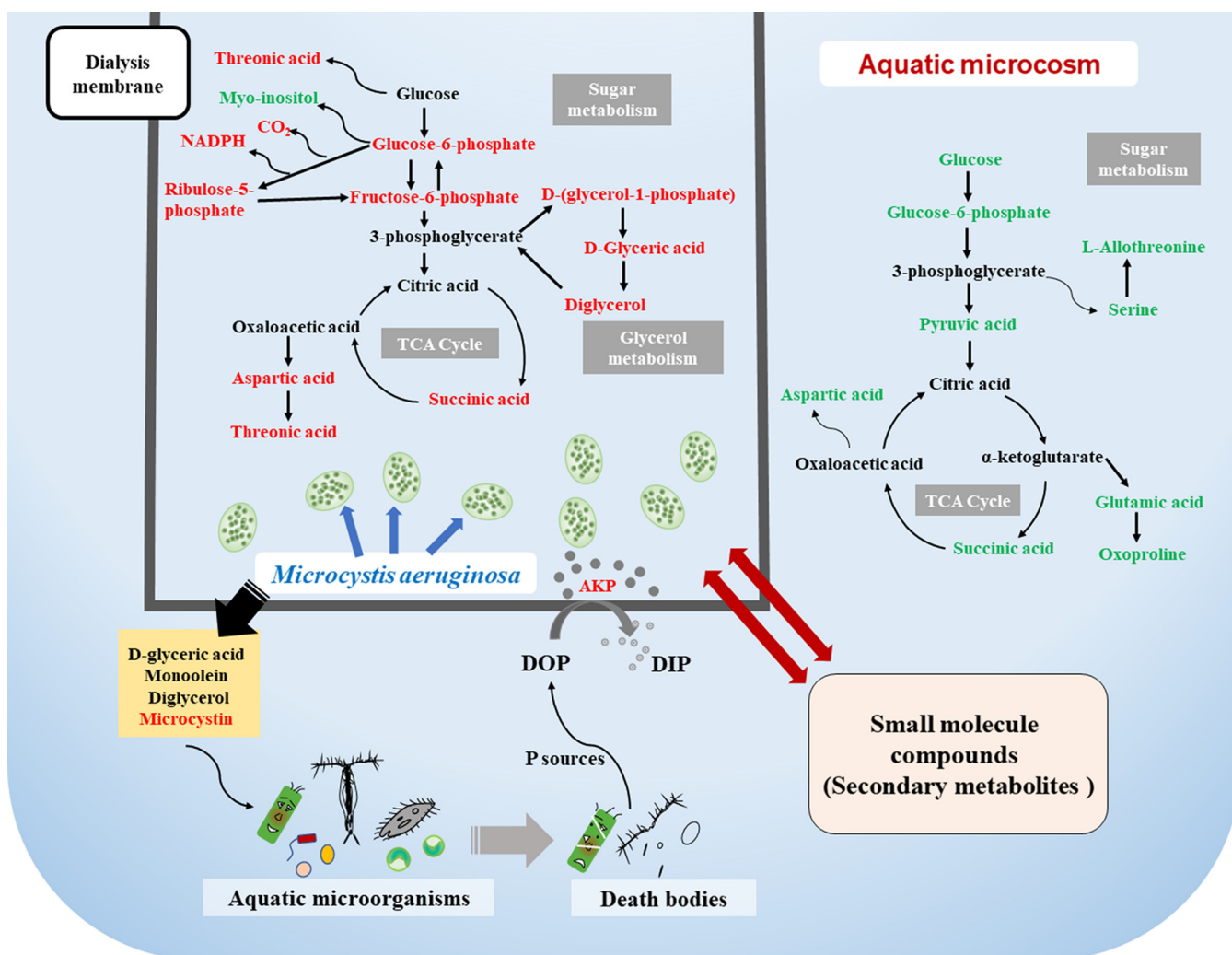
FIG 8 Schematic diagram of changes in *M. aeruginosa* and microbial communities after coculture treatment. Red represents the upregulation of the metabolites in the treatment group compared to that in the control group, and blue and green represent the downregulation of metabolites.

during its growth. *M. aeruginosa* slightly decreased bacterial microbial community diversity and abundance but had a more significant impact on the diversity and abundance of eukaryotes. Furthermore, some metabolites released from *M. aeruginosa* or from *M. aeruginosa* lysis could be harmful to biota and negatively affect the growth of algal competitors or predators, which could be the key factor to enable this opportunistic group of photosynthetic prokaryotes to thrive in a wide range of habitats.

MATERIALS AND METHODS

Aquatic microcosms and *M. aeruginosa* culture. Water samples were collected in sterile containers during the bloom-free phase from Meiliang Bay on Lake Taihu (30°55′40″ to 31°32′58″N; 119°52′32″ to 120°36′10″E), a location where the water quality is monitored monthly, in November 2017. Microorganisms first isolated from Lake Taihu received sterile BG-11 nutrient medium (initial pH 7.1; for the chemical composition, see Table S1 in the supplemental material) (28). An axenic culture of *M. aeruginosa* (strain FACHB-905) obtained from the Institute of Hydrobiology (Chinese Academy of Sciences, Wuhan, China) was also grown on sterilized BG-11 liquid medium. All cultures were incubated in an environmental chamber at $25 \pm 0.5°C$ under cool-white fluorescent illumination (46 μmol/m²/s, 12 h light/12 h dark).

Coculture experimental design. A coculture design was used to investigate the interactions between axenic *M. aeruginosa* and aquatic microorganisms. Sterile permeable dialysis cellulose membrane tubing (Economical Biotech membrane 14 KD, 77-mm width; Sangon Biotech, Shanghai, China) was used to isolate *M. aeruginosa* and lake water microbial communities from each other. This design allowed for the exudation of small molecule compounds through the dialysis membrane and prevented cell contact between *M. aeruginosa* and naturally occurring microbial populations (51).

Prior to incubation, both microorganisms and *M. aeruginosa* (which reached approximately 10^7 cells/ml) were harvested by centrifugation (8,000 $\times$ *g* for 10 min, 4°C) and washed several times with ultrapure water. The microorganisms and *M. aeruginosa* were cultured in modified BG-11 (NaNO$_3$, 10 mg/liter; K$_2$HPO$_4$, 1 mg/liter) for 1 day to allow them to adapt to experimental conditions, in which nitrate nitrogen (NO$_3^-$-N) and DIP were added at concentrations representative of ambient Lake Taihu water. Three groups of experiments were carried out to observe the growth of *M. aeruginosa* and associated aquatic microorganisms. (i) For the coculture group, an axenic dialysis bag filled with 180 ml of *M. aeruginosa* culture (Treat-Ma) was submerged in 900 ml of aquatic microorganism culture (Treat-AM) and cocultured in a sterilized 2,000-ml glass beaker. (ii) For control group 1, a dialysis bag filled with 180 ml of *M. aeruginosa* culture (*M. aeruginosa* control group, Con-Ma) was submerged in 900 ml of *M. aeruginosa*-containing medium. Because 900 ml of aquatic microorganisms were added outside the dialysis bag in the coculture group, 900 ml of *M. aeruginosa* culture was also added to submerge the dialysis bag in the monoculture group in order to maintain culture conditions consistent with the coculture group. Samples for analysis were collected only from the 180-ml dialysis bag. (iii) For control group 2 (similar to control 1), a dialysis bag filled with 180 ml of aquatic microorganism-containing medium was submerged in 900 ml of aquatic microorganism culture (i.e., the aquatic microorganism control group [Con-AM]).

The initial cell density was calculated as the OD$_{680}$. For the microcosm, an OD$_{680}$ of 0.03 was selected; this was similar to the value for water samples collected from Lake Taihu. For *M. aeruginosa*, preliminary experiments were conducted with OD$_{680}$s of 0.03, 0.06, and 0.09 (approximately 1.72 $\times$ 10^5, 3.44 $\times$ 10^5, and 5.16 $\times$ 10^5 cells/ml, respectively), which were of the same orders of magnitude as cell densities measured in Lake Taihu during the water bloom phase (13). The results showed that the similar inhibitory effects of *M. aeruginosa* on aquatic microorganisms among the 0.03-, 0.06-, and 0.09-OD$_{680}$ groups were statistically significant (see Fig. S1 in the supplemental material). Therefore, the OD$_{680}$s of both *M. aeruginosa* and the microcosm were selected as 0.03. The entire experimental process is shown in Fig. 1A.

Measurements of *M. aeruginosa* and microbial growth and physicochemical water quality parameters. The growth status of *M. aeruginosa* and associated microorganisms was monitored daily by spectrophotometry. In addition, the cell density of *M. aeruginosa* was measured by cell counting, whereas the concentration of Chl-a represented the total phytoplankton biomass in the microcosm (2). During coculture, the cell number and the OD$_{680}$ of *M. aeruginosa* and chlorophyll *a* (Chl-a) and the OD$_{680}$ of the microcosm were measured every 24 h. The initially cultured *M. aeruginosa* was enumerated microscopically to establish a linear regression equation between the number of cells ($y \times 10^5$ cells/ml) and OD$_{680}$ (*x*). The number of cells was calculated based on the equation $y = 34.1x + 0.7$ ($R^2 = 99.17$). A series of water quality parameters was measured as follows. The pH was measured using a pH meter (FE-20; Mettler Toledo, Columbus, OH). The electrical conductivity (EC) was measured using an EC meter (InPro 7100i/12/120; Mettler Toledo, Zurich, Switzerland). The dissolved oxygen (DO) was measured using a DO meter (Visiferm DO120; Hamilton Bonaduz, Zurich, Switzerland). The NO$_3^-$-N, total phosphorus (TP), and DIP were measured by UV spectrophotometry, ammonium molybdate spectrophotometry, and molybdenum rhenium spectrophotometry, respectively (52, 53). Alkaline phosphatase (AKP) assays were performed using a commercial kit (Suzhou Comin Biotechnology Co., Ltd., Suzhou, China). AKP can hydrolyze a natural phospholipid monoester complex and catalyze the formation of free phenol from sodium phenyl phosphate. Phenol reacts with 4-aminoantipyrine and potassium ferricyanide to form derivatives with characteristic light absorption at 510 nm.

DNA extraction, amplification and sequencing, and analysis of microbially diverse populations. At 4 and 8 days of culture incubation, samples were collected from control (Con-AM4 and Con-AM8, respectively) and coculture microcosms (Treat-AM4 and Treat-AM8, respectively) for DNA extraction using a MoBio PowerSoil DNA isolation kit (Mo Bio Laboratories, Inc., Carlsbad, CA). Extracted DNA was used for Illumina 16S rRNA/18S rRNA gene amplicon sequencing. The V3-V4 region of the 16S rRNA gene was amplified using the primers 341F (CCTAYGGGRBGCASCAG) and 806R (GGACTACNNGGGTATCTAAT), and the V4 region of the 18S rRNA gene was amplified using the primers 528F (GCGGTAATTCCAGCTC CAA) and 706R (AATCCRAGAATTTCACCTCT). Each group was amplified in triplicate. All PCRs were carried out with Phusion High-Fidelity PCR master mix (Thermo Fisher Scientific, Basel, Switzerland). Sequencing libraries were generated by using a TruSeq DNA PCR-free sample preparation kit (Illumina, San Diego, CA) according to the manufacturer's recommendations, and index codes were added. The library quality was assessed on a Qubit 2.0 fluorometer (Thermo Fisher Scientific, Carlsbad, CA) and an Agilent 2100 bioanalyzer (Agilent, Palo Alto, CA). Lastly, the library was sequenced on the Illumina HiSeq 2500 platform, and 250-bp paired-end reads were generated. Microbial diversity was computed using QIIME (v1.6.0). The operational taxonomic units (OTUs; the number of species normalized to the abundance of 16S rRNA/18S rRNA genes) were computed for each treatment. The OTUs in samples were aligned with the SILVA database to classify the microbial community into phylotypes.

Metabolomic analyses. At 8 days of incubation, approximately 0.3 g of *M. aeruginosa* (Con-Ma and Treat-Ma), microorganism samples (Con-AM and Treat-AM) and culture medium (Con-AMW and Treat-AMW) were collected from coculture and monoculture systems for metabolomic analysis. *M. aeruginosa* or a microorganism sample was transferred to a 4-ml glass bottle with 20 μl of internal standard (2-chloro-L-phenylalanine dissolved in methanol) and 600 μl of a mixture of methanol and water (4/1, vol/vol). Chloroform (200 μl) was added before ultrasonic homogenization in an ice bath (500 W, 6 min, 6 s on, 4 s off). Samples were then centrifuged at 10,000 $\times$ *g* for 15 min, and supernatants were collected for further purification. The culture medium was filtered on 0.7-μm-pore-size Whatman GF/F fiberglass filters at 0.1 MPa, and the filtrates were collected for metabolomic analysis. The supernatant (600 μl) in a glass vial was dried in a centrifugal concentrating freeze dryer, followed by the addition of 80 μl of

pyridine (containing 15 mg/ml methoxyamine hydrochloride). The resultant mixture was vortexed vigorously for 2 min, followed by incubation at 37°C for 90 min. BSTFA [bis(trimethylsilyl) trifluoroacetamide] (80 μl, with 1% TMCS [trimethyl chlorosilane]) and 20 μl of n-hexane were added to the mixture, which was then vortexed vigorously for 2 min and derivatized at 70°C for 60 min. The derivatized samples were analyzed on an Agilent 7890A gas chromatograph coupled to an Agilent 5975C MSD system. An HP-5MS fused-silica capillary column (30 m by 0.25 mm by 0.25 μm; Agilent J&W, Palo Alto, CA) was utilized to separate the derivative. Finally, all MS data were analyzed using ChromaTOF software (v 4.34; LECO, St. Joseph, MI).

Quantification of MCs in culture medium. To measure the MCs in the medium, water was collected from aquatic microcosms in 1.5-ml tubes and centrifuged at 10,000 $\times$ g for 10 min at 4°C. The supernatants were then assayed for MC content using a Beacon MC plate kit according to the manufacturer's instructions. The Beacon microcystin plate kit uses a polyclonal antibody that binds both microcystins and a microcystin-enzyme conjugate for a limited number of antibody-binding sites, which, however, cannot differentiate between MC-LR and other MC variants.

Statistical analyses. Statistical significance among biochemical and physiological measurement data was tested using one-way analysis of variance (StatView 5.0; SAS Institute, Cary, NC). Differences were considered statistically significant when the P value was <0.05. Metabolomics data sets were normalized to the total peak area of each sample in Excel 2007 (Microsoft) and imported into SIMCA (v14.0; Umetrics, Umeå, Sweden). Each sample was taken from a different culture. The metabolomics analysis was set up in six replicates, and the remaining experiments were set up in triplicate. All samples were taken at approximately 9 a.m. Data are presented as means $\pm$ the standard errors of the mean (SEM).

Data availability. The 16S and 18S rRNA gene sequence data generated in this study are available in the NCBI Sequence Read Archive (SRA) under accession numbers SAMN12388980 to SAMN12388991 (16S) and SAMN12394199 to SAMN12394210 (18S).

SUPPLEMENTAL MATERIAL

Supplemental material for this article may be found at https://doi.org/10.1128/AEM .01362-19.

SUPPLEMENTAL FILE 1, PDF file, 0.7 MB.
SUPPLEMENTAL FILE 2, XLS file, 0.03 MB.

REFERENCES

1. Scheffer M, Carpenter S, Foley JA, Folke C, Walker B. 2001. Catastrophic shifts in ecosystems. Nature 413:591–596. https://doi.org/10.1038/ 35098000.
2. Pace ML, Batt RD, Buelo CD, Carpenter SR, Cole JJ, Kurtzweil JT, Wilkinson GM. 2017. Reversal of a cyanobacterial bloom in response to early warnings. Proc Natl Acad Sci U S A 114:352–357. https://doi.org/10.1073/ pnas.1612424114.
3. Paerl HW, Otten TG. 2013. Harmful cyanobacterial blooms: causes, consequences, and controls. Microb Ecol 65:995–1010. https://doi.org/10 .1007/s00248-012-0159-y.
4. Otten TG, Paerl HW, Dreher TW, Kimmerer WJ, Parker AE. 2017. The molecular ecology of *Microcystis sp.* blooms in the San Francisco estuary. Environ Microbiol 19:3619–3637. https://doi.org/10.1111/1462-2920.13860.
5. Paerl HW. 2008. Nutrient and other environmental controls of harmful cyanobacterial blooms along the fresh water marine continuum. Adv Exp Med Biol 619:217–237. https://doi.org/10.1007/978-0-387-75865-7_10.
6. Ren L, Wang P, Wang C, Chen J, Hou J, Qian J. 2017. Algal growth and utilization of phosphorus studied by combined monocultures and co-culture experiments. Environ Pollut 220:274–285. https://doi.org/10 .1016/j.envpol.2016.09.061.
7. Paerl HW, Xu H, McCarthy MJ, Zhu G, Qin B, Li Y, Gardner WS. 2011. Controlling harmful cyanobacterial blooms in a hyper-eutrophic lake (Lake Taihu, China): the need for a dual nutrient (N and P) management strategy. Water Res 45:1973–1983. https://doi.org/10.1016/j.watres.2010 .09.018.
8. Paerl HW, Huisman J. 2008. Blooms like it hot. Science 320:57–58. https://doi.org/10.1126/science.1155398.
9. Lewis WM, Wurtsbaugh WA, Paerl HW. 2011. Rationale for control of anthropogenic nitrogen and phosphorus to reduce eutrophication of inland waters. Environ Sci Technol 45:10300–10305. https://doi.org/10 .1021/es202401p.
10. Saxton MA, Arnold RJ, Bourbonniere RA, McKay RM, Wilhelm SW. 2012. Plasticity of total and intracellular phosphorus quotas in *Microcystis aeruginosa* cultures and Lake Erie algal assemblages. Front Microbiol 3:3–11. https://doi.org/10.3389/fmicb.2012.00003.
11. Harke MJ, Davis TW, Watson SB, Gobler CJ. 2016. Nutrient-controlled niche differentiation of western lake Erie cyanobacterial populations revealed via metatranscriptomic surveys. Environ Sci Technol 50: 604–615. https://doi.org/10.1021/acs.est.5b03931.
12. Paerl HW, Otten TG. 2016. Duelling "CyanoHABs": unravelling the environmental drivers controlling dominance and succession among diazotrophic and non-N$_2$-fixing harmful cyanobacteria. Environ Microbiol 18:316–324. https://doi.org/10.1111/1462-2920.13035.
13. Song H, Lavoie M, Fan X, Tan H, Liu G, Xu P, Fu Z, Paerl HW, Qian H. 2017. Allelopathic interactions of linoleic acid and nitric oxide increase the competitive ability of *Microcystis aeruginosa*. ISME J 11:1865–1876. https://doi.org/10.1038/ismej.2017.45.
14. Liu G, Ke M, Fan X, Zhang M, Zhu Y, Lu T, Sun L, Qian H. 2018. Reproductive and endocrine-disrupting toxicity of *Microcystis aeruginosa* in female zebrafish. Chemosphere 192:289–296. https://doi.org/10.1016/ j.chemosphere.2017.10.167.
15. Qian H, Zhang M, Liu G, Lu T, Sun L, Pan X. 2019. Effects of different concentrations of *Microcystis aeruginosa* on the intestinal microbiota and immunity of zebrafish (*Danio rerio*). Chemosphere 214:579–586. https://doi.org/10.1016/j.chemosphere.2018.09.156.
16. Qian H, Xu J, Lu T, Zhang Q, Qu Q, Yang Z, Pan X. 2018. Responses of unicellular alga *Chlorella pyrenoidosa* to allelochemical linoleic acid. Sci Total Environ 625:1415–1422. https://doi.org/10.1016/j.scitotenv.2018 .01.053.
17. Liu L, Chen H, Liu M, Yang JR, Xiao P, Wilkinson M, Yang J. 2019. Response of the eukaryotic plankton community to the cyanobacterial

biomass cycle over 6 years in two subtropical reservoirs. ISME J 13: 2196–2208. https://doi.org/10.1038/s41396-019-0417-9.

18. Liu M, Liu L, Chen H, Zheng Y, Yang JR, Xue Y, Huang B, Yang J. 2019. Community dynamics of free-living and particle-attached bacteria following a reservoir *Microcystis* bloom. Sci Total Environ 660:501–511. https://doi.org/10.1016/j.scitotenv.2018.12.414.

19. Tang X, Gao G, Chao J, Wang X, Zhu G, Qin B. 2010. Dynamics of organic-aggregate-associated bacterial communities and related environmental factors in Lake Taihu, a large eutrophic shallow lake in China. Limnol Oceanogr 55:469–480. https://doi.org/10.4319/lo.2009.55.2.0469.

20. Wilhelm SW, Farnsley SE, Lecleir GR, Layton AC, Satchwell MF, Debruyn JM, Boyer GL, Zhu G, Paerl HW. 2011. The relationships between nutrients, cyanobacterial toxins and the microbial community in Taihu (Lake Tai), China. Harmful Algae 10:207–215. https://doi.org/10.1016/j.hal.2010.10.001.

21. Ullah H, Nagelkerken I, Goldenberg SU, Fordham DA. 2018. Climate change could drive marine food web collapse through altered trophic flows and cyanobacterial proliferation. PLoS Biol 16:e2003446. https://doi.org/10.1371/journal.pbio.2003446.

22. DeMott WR, Gulati RD, Van Donk E. 2001. Daphnia food limitation in three hypereutrophic Dutch lakes: evidence for exclusion of large-bodied species by interfering filaments of cyanobacteria. Limnol Oceanogr 46:2054–2060. https://doi.org/10.4319/lo.2001.46.8.2054.

23. Paerl HW. 1988. Nuisance phytoplankton blooms in coastal, estuarine, and inland waters. Limnol Oceanogr 33:823–847. https://doi.org/10.4319/lo.1988.33.4_part_2.0823.

24. Brauer VS, Stomp M, Bouvier T, Fouilland E, Leboulanger C, Confurius-Guns V, Weissing FJ, Stal L, Huisman J. 2015. Competition and facilitation between the marine nitrogen-fixing cyanobacterium *Cyanothece* and its associated bacterial community. Front Microbiol 5:795. https://doi.org/10.3389/fmicb.2014.00795.

25. Hmelo LR, van Mooy BAS, Mincer RJ. 2012. Characterization of bacterial epibionts on the cyanobacterium *Trichodesmium*. Aquat Microb Ecol 67:1–14. https://doi.org/10.3354/ame01571.

26. de Figueiredo DR, Reboleira A, Antunes SC, Abrantes N, Azeiteiro U, Goncalves F, Pereira MJ. 2006. The effect of environmental parameters and cyanobacterial blooms on phytoplankton dynamics of a Portuguese temperate lake. Hydrobiologia 568:145–157. https://doi.org/10.1007/s10750-006-0196-y.

27. Jones BI. 1987. Lake Okeechobee eutrophication research and management. Aquatics 9:21–26.

28. Lu T, Zhu Y, Ke M, Peijnenburg WJGM, Zhang M, Wang T, Chen J, Qian H. 2019. Evaluation of the taxonomic and functional variation of freshwater plankton communities induced by trace amounts of the antibiotic ciprofloxacin. Environ Int 126:268–278. https://doi.org/10.1016/j.envint.2019.02.050.

29. Klase G, Lee S, Liang S, Kim J, Zo YG, Lee J. 2019. The microbiome and antibiotic resistance in integrated fishfarm water: implications of environmental public health. Sci Total Environment 649:1491–1501. https://doi.org/10.1016/j.scitotenv.2018.08.288.

30. Sebastian M, Ammerman JW. 2009. The alkaline phosphatase PhoX is more widely distributed in marine bacteria than the classical PhoA. ISME J 3:563–572. https://doi.org/10.1038/ismej.2009.10.

31. Paerl HW, Millie DF. 1996. Physiological ecology of toxic cyanobacteria. Phycologia 35:160–167. https://doi.org/10.2216/i0031-8884-35-6S-160.1.

32. Sukenik A, Quesada A, Salmaso N. 2015. Global expansion of toxic and nontoxic cyanobacteria: effect on ecosystem functioning. Biodivers Conserv 24:889–908. https://doi.org/10.1007/s10531-015-0905-9.

33. Qian H, Zhu Y, Chen S, Jin Y, Lavoie M, Ke M, Fu Z. 2018. Interacting effect of diclofop-methyl on the rice rhizosphere microbiome and denitrification. Pesticide Biochem Physiol 146:90–96. https://doi.org/10.1016/j.pestbp.2018.03.002.

34. Te SH, Tan BF, Thompson JR, Gin KY. 2017. Relationship of microbiota and cyanobacterial secondary metabolites in planktothricoides-dominated bloom. Environ Sci Technol 51:4199–4209. https://doi.org/10.1021/acs.est.6b05767.

35. Haraldsson M, Gerphagnon M, Bazin P, Colombet J, Tecchio S, Sime-Ngando T, Niquil N. 2018. Microbial parasites make cyanobacteria blooms less of a trophic dead end than commonly assumed. ISME J 12:1008–1020. https://doi.org/10.1038/s41396-018-0045-9.

36. Xue Y, Chen H, Yang JR, Liu M, Huang B, Yang J. 2018. Distinct patterns and processes of abundant and rare eukaryotic plankton communities

37. following a reservoir cyanobacterial bloom. ISME J 12:2263–2277. https://doi.org/10.1038/s41396-018-0159-0.

37. Zhang HL, Du WC, Peralta-Videa JR, Gardea-Torresdey JL, White JC, Keller A, Guo HY, Ji R, Zhao LJ. 2018. Metabolomics reveals how cucumber (*Cucumis sativus*) reprograms metabolites to cope with silver ions and silver nanoparticle-induced oxidative stress. Environ Sci Technol 52: 8016–8026. https://doi.org/10.1021/acs.est.8b02440.

38. Welkie DG, Rubin BE, Diamond S, Hood RD, Savage DF, Golden SS. 2019. A hard day's night: cyanobacteria in diel cycles. Trends Microbiol 27: 231–242. https://doi.org/10.1016/j.tim.2018.11.002.

39. Stincone A, Prigione A, Cramer T, Wamelink MMC, Campbell K, Cheung E, Olin-Sandoval V, Grüning N-M, Krüger A, Tauqeer Alam M, Keller MA, Breitenbach M, Brindle KM, Rabinowitz JD, Ralser M. 2015. The return of metabolism: biochemistry and physiology of the pentose phosphate pathway. Biol Rev 90:927–963. https://doi.org/10.1111/brv.12140.

40. Zhao L, Huang Y, Adeleye AS, Keller AA. 2017. Metabolomics reveals $Cu(OH)_2$ nanopesticide-activated anti-oxidative pathways and decreased beneficial antioxidants in spinach leaves. Environ Sci Technol 51: 10184–10194. https://doi.org/10.1021/acs.est.7b02163.

41. Zhang H, Zhao Z, Kang P, Wang Y, Feng J, Jia J, Zhang Z. 2018. Biological nitrogen removal and metabolic characteristics of a novel aerobic denitrifying fungus *Hanseniaspora uvarum* strain KPL108. Bioresour Technol 267:569–577. https://doi.org/10.1016/j.biortech.2018.07.073.

42. Tanabe Y, Hodoki Y, Sano T, Tada K, Watanabe MM. 2018. Adaptation of the freshwater bloom-forming cyanobacterium *Microcystis aeruginosa* to brackish water is driven by recent horizontal transfer of sucrose genes. Front Microbiol 9:1150. https://doi.org/10.3389/fmicb.2018.01150.

43. Zhao L, Huang Y, Paglia K, Vaniya A, Wancewicz B, Keller AA. 2018. Metabolomics reveals the molecular mechanisms of copper induced cucumber leaf (*Cucumis sativus*) senescence. Environ Sci Technol 52: 7092–7100. https://doi.org/10.1021/acs.est.8b00742.

44. Waal DBVD, Ferreruela G, Tonk L, Donk EV, Huisman J, Visser PM, Matthijs HCP. 2010. Pulsed nitrogen supply induces dynamic changes in the amino acid composition and microcystin production of the harmful cyanobacterium *Planktothrix agardhii*. FEMS Microbiol Ecol 74:430–438. https://doi.org/10.1111/j.1574-6941.2010.00958.x.

45. Hartmann J, Albert A, Ganzera M. 2015. Effects of elevated ultraviolet radiation on primary metabolites in selected alpine algae and cyanobacteria. J Photochem Photobiol B Biol 149:149–155. https://doi.org/10.1016/j.jphotobiol.2015.05.016.

46. Dai R, Liu H, Qu J, Zhao X, Hou Y. 2009. Effects of amino acids on microcystin production of the *Microcystis aeruginosa*. J Hazard Mater 161:730–736. https://doi.org/10.1016/j.jhazmat.2008.04.015.

47. Cao DD, Zhang CP, Zhou K, Jiang YL, Tan XF, Xie J, Ren YM, Chen Y, Zhou CZ, Hou WT. 2019. Structural insights into the catalysis and substrate specificity of cyanobacterial aspartate racemase McyF. Biochem Biophys Res Commun 514:1108–1114. https://doi.org/10.1016/j.bbrc.2019.05.063.

48. Ganem-Quintanar A, Quintanar-Guerrero D, Buri P. 2000. Monoolein: a review of the pharmaceutical applications. Drug Dev Ind Pharm 26: 809–820. https://doi.org/10.1081/DDC-100101304.

49. da Silva GP, Mack M, Contiero J. 2009. Glycerol: a promising and abundant carbon source for industrial microbiology. Biotechnol Adv 27: 30–39. https://doi.org/10.1016/j.biotechadv.2008.07.006.

50. Zilliges Y, Kehr JC, Meissner S, Ishida K, Mikkat S, Hagemann M, Kaplan A, Börner T, Dittmann E. 2011. The cyanobacterial hepatotoxin microcystin binds to proteins and increases the fitness of *Microcystis* under oxidative stress conditions. PLoS One 6:e17615. https://doi.org/10.1371/journal.pone.0017615.

51. Poulsonellestad KL, Jones CM, Roy J, Viant MR, Fernández FM, Kubanek J, Nunn BL. 2014. Metabolomics and proteomics reveal impacts of chemically mediated competition on marine plankton. Proc Natl Acad Sci U S A 111:9009–9014. https://doi.org/10.1073/pnas.1402130111.

52. Song H, Xu J, Lavoie M, Fan X, Liu G, Sun L, Fu Z, Qian H. 2017. Biological and chemical factors driving the temporal distribution of cyanobacteria and heterotrophic bacteria in a eutrophic lake (West Lake, China). Appl Microbiol Biotechnol 101:1685–1696. https://doi.org/10.1007/s00253-016-7968-8.

53. Fan X, Xu J, Lavoie M, Peijnenburg W, Zhu Y, Lu T, Fu Z, Zhu T, Qian H. 2018. Multiwall carbon nanotubes modulate paraquat toxicity in *Arabidopsis thaliana*. Environ Pollut 233:633–641. https://doi.org/10.1016/j.envpol.2017.10.116.